

## Second Taylor vortex flow: Effects of radius ratio and aspect ratio

Q. Xiao, T. T. Lim, and Y. T. Chew

Citation: *Physics of Fluids* (1994-present) **14**, 1537 (2002); doi: 10.1063/1.1452475

View online: <http://dx.doi.org/10.1063/1.1452475>

View Table of Contents: <http://scitation.aip.org/content/aip/journal/pof2/14/4?ver=pdfcov>

Published by the [AIP Publishing](#)

---

### Articles you may be interested in

[The onset of steady vortices in Taylor-Couette flow: The role of approximate symmetry](#)

*Phys. Fluids* **24**, 064102 (2012); 10.1063/1.4726252

[Effects of weak elasticity on the stability of high Reynolds number co- and counter-rotating Taylor-Couette flows](#)

*J. Rheol.* **55**, 1271 (2011); 10.1122/1.3626584

[Linear stability of cylindrical Couette flow in the convection regime](#)

*Phys. Fluids* **17**, 054112 (2005); 10.1063/1.1905482

[Interaction of wavy cylindrical Couette flow with endwalls](#)

*Phys. Fluids* **16**, 1140 (2004); 10.1063/1.1652671

[Interaction between Ekman pumping and the centrifugal instability in Taylor–Couette flow](#)

*Phys. Fluids* **15**, 467 (2003); 10.1063/1.1534108

---



### Vacuum Solutions from a Single Source

- Turbopumps
- Backing pumps
- Leak detectors
- Measurement and analysis equipment
- Chambers and components

**PFEIFFER**  **VACUUM**

## Second Taylor vortex flow: Effects of radius ratio and aspect ratio

Q. Xiao, T. T. Lim, and Y. T. Chew

*Department of Mechanical Engineering, National University of Singapore, 10 Kent Ridge Crescent, Singapore 119260*

(Received 24 May 2001; accepted 2 January 2002; published 7 March 2002)

This paper is motivated by our earlier investigation on the stability of Taylor–Couette flow in which we discovered a previously unidentified flow regime, which we refer to as “Second Taylor vortex flow” (STVF) when an inner cylinder is subjected to some critical acceleration [Lim, Chew, and Xiao, *Phys. Fluids* **10**, 3233 (1998)]. The aim here is to explore how the STVF regime is affected by changes in radius ratio and aspect ratio. Results show that the STVF regime is sensitive to the gap size between the two cylinders, and does not exist for some radius ratios, whereas it increases with decreasing aspect ratio. © 2002 American Institute of Physics. [DOI: 10.1063/1.1452475]

Recently, we conducted a systematic investigation on the effect of acceleration on the stability of Taylor–Couette flow,<sup>1</sup> by subjecting the inner cylinder to a wide range of acceleration and keeping the outer one stationary. The results showed that if the acceleration ( $d\text{Re}/dt$ ) was below a certain critical value, the flow state transition followed the classical sequence from circular Couette flow (CCF)  $\Rightarrow$  Taylor vortex flow (TVF)  $\Rightarrow$  wavy vortex flow (WVF)  $\Rightarrow$  turbulent vortex flow as the Reynolds number was increased (see Fig. 1 of Ref. 1). However, above the critical acceleration, we found a previously unidentified flow regime, which we referred to as “second Taylor vortex flow” (or STVF for short). An interesting feature of this flow regime is that the Taylor vortices are axisymmetric and do not display any wavy motion even though the regime is located inside the wavy flow regime under quasi-steady condition (i.e.,  $1.85\text{Re}_c < \text{Re} < 3.01\text{Re}_c$ ). Since our earlier study was restricted to only one radius ratio and one aspect ratio ( $\eta=0.803$ ,  $\Gamma=50.54$ ), this motivated us to carry out the present investigation to explore how the STVF regime is affected by changes in the radius ratio and aspect ratio.

The experiments are conducted using the same apparatus as in our previous investigation.<sup>1</sup> It consists of a stationary outer cylinder of radius  $R_2$ , and a rotating inner concentric cylinder of radius  $R_1$ , which is controlled by a PC through a micro-stepper motor. During assembly, great care was taken to ensure that the two cylinders are concentric and accurately aligned.

To examine the effect of radius ratio, we vary the diameter of the inner cylinder while keeping the outer one fixed at 94.0 mm. The three inner radii ( $R_1$ ) used are 62.0 mm, 75.5 mm, and 84.0 mm, which give the radius ratio ( $\eta = R_1/R_2$ ) of 0.660, 0.803, and 0.894, respectively. The aspect ratio ( $\Gamma = H/d$ ) is maintained at 30, where  $H$  is the height of the fluid column and  $d$  is the gap size between the two cylinders. Similarly, to study the effect of aspect ratio, we vary  $H$  while keeping the radius ratio ( $\eta$ ) constant at 0.803. The five aspect ratios considered are 15, 20, 25, 30, and 50.54. One end of the fluid column is bounded by a stationary solid surface while the other end is a free liquid

surface. This configuration is similar to that used by Cole<sup>2</sup> to investigate the annulus-length effects on Taylor-vortex instability. The height of the fluid column is accurately measured using a cathetometer, and the kinematic viscosity ( $\nu$ ) of the working solution, which is glycerine–water mixture of a predetermined proportion, is measured using a HAAKE Rheometer at the room temperature of 27 °C. All the experiments are conducted in an air-conditioned room, where the temperature variation is less than 0.5 °C throughout the experiment.

To visualize the flow, Kalliroscope AQ-100 reflective flakes are added to the working solution and illuminated by five 30 W fluorescent lamps and two spotlights. To determine whether the flow is nonvortical versus vortical versus wavy flow, a thin laser sheet, obtained by expanding a 5 watt argon ion laser beam through a 8 mm cylindrical lens, is used to illuminate the mid-section of the annulus, and the resulting vortex motions are captured using a CCD video camera for subsequent analysis. During slow motion video replay, Taylor vortices appear as a series of counter rotating “vortex cells” which appear “stationary” if the vortices are axisymmetric and nonwavy, and they display an oscillating motion if the vortices are wavy.

Besides the radius ratio and aspect ratio, the other two important parameters are the Reynolds number ( $\text{Re} = R_1\Omega/\nu$ ) and the acceleration. The latter is expressed nondimensionally as  $d\text{Re}/dt^* = (R_1d/\nu)d\Omega/dt^*$ , where  $t^*$  is a nondimensional time defined as  $t\nu/d^2$ , and  $d^2/\nu$  is the radial diffusion time. This definition is different from that in our previous study<sup>1</sup> where the acceleration was expressed as  $[d\text{Re}/dt = (R_1d/\nu)d\Omega/dt]$ , which has the dimension of time. In all cases, the inner cylinder is accelerated from rest up to a desired speed ( $\Omega$ ) over a predetermined time-interval, and then left to rotate at the final speed for more than two hours before the results are taken. In terms of radial diffusion time, two hours is equivalent to approximately  $50(d^2/\nu)$  in the case of  $\eta=0.660$ , and is considerably higher for the other two higher radius ratio cases. To avoid any possible “memory effect” of the fluid, the time interval between each experiment is kept more than one hour apart.

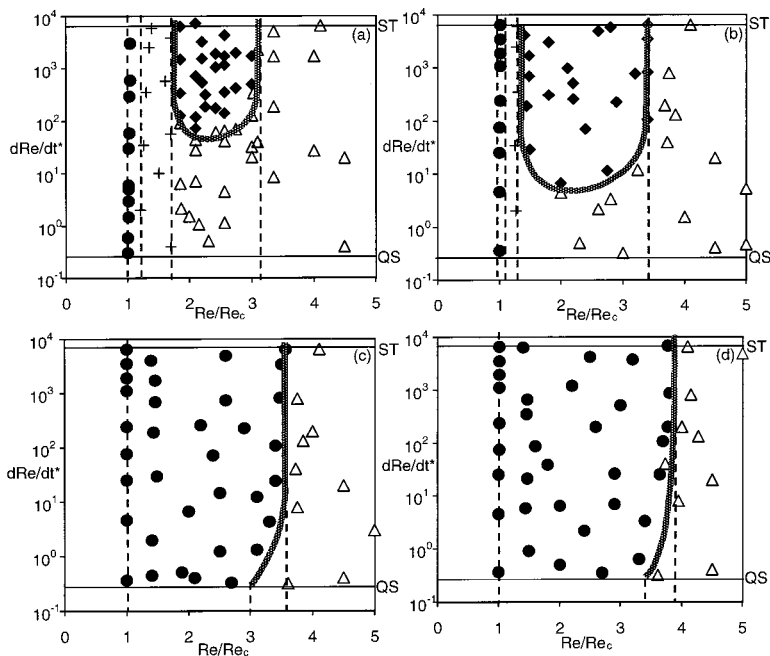


FIG. 1. Effect of aspect ratio on the STVF regime. (a)  $\Gamma=50.54$ . (b)  $\Gamma=25$ . (c)  $\Gamma=20$ . (d)  $\Gamma=15$ . ●: Taylor vortex flow; ◆: Second Taylor vortex flow; +: Laminar wavy vortex flow ( $m=2$ ); △: Laminar wavy vortex flow ( $m=3$ ).  $t^*$  is defined here as  $t^*=t\nu/d^2$ . The top and the bottom horizontal lines indicated by ST and QS represent the sudden start and quasi-steady conditions, respectively.

For ease of reference, the upper limit of the acceleration, which is dictated by the inertia of the system, is referred to as the “sudden start” condition and the lower limit is referred to as “quasi-steady” condition, and they correspond to  $dRe/dt \approx 200$  ( $s^{-1}$ ) and  $dRe/dt \approx 0.01$  ( $s^{-1}$ ), respectively. Since the equivalent nondimensional acceleration ( $dRe/dt^*$ ) is a function of the gap size ( $d$ ), they are clearly identified for each radius ratio in the figure. Using the method described in Holman,<sup>3</sup> the experimental uncertainties for the Reynolds number and nondimensional acceleration ( $dRe/dt^*$ ) are 2.55% and 3.6%, respectively.

To verify the accuracy of our experimental set-up, tests are carried out to determine the critical Reynolds number for the onset of Taylor vortices ( $Re_c$ ) under quasi-steady condition, and our results for the three radius ratios are in very good agreement with the theoretical result of Taylor,<sup>4</sup> and the experimental results of DiPrima *et al.*,<sup>5</sup> and Debler *et al.*<sup>6</sup>

The present results show that STVF regime is sensitive to changes in the radius ratio and aspect ratio. Among the three radius ratios investigated, STVF regime is found to exist in  $\eta=0.803$  only, and not in  $\eta=0.660$  and  $\eta=0.894$ . Because of the space constraint, detailed experimental data are not presented here, and can be obtained from Ref. 7. Nevertheless, what is important is that the STVF regime is also bounded by a parabolic-like curve similar to that displayed in Fig. 1 of Ref. 1, except for a slightly lower critical acceleration for the onset of the STVF, and a shift in the upper and lower limits of the Reynolds number, which can be attributed to a lower aspect ratio used in the present study. In the case of  $\eta=0.894$ , the flow state transition follows the classical sequence (i.e., from CCF  $\Rightarrow$  TVF  $\Rightarrow$  WVF) as the Reynolds number is increased, and is independent of the acceleration. Moreover, the TVF regime occupies only a very narrow range from  $Re/Re_c=1$  to  $Re/Re_c \approx 1.2$  before the flow transition to WVF. However, when the radius ratio is reduced to  $\eta=0.660$ , there is a considerable expansion of the TVF

regime with the upper limit extending to  $Re/Re_c=8.2$ , which is almost eight times larger than that in  $\eta=0.894$ . Interestingly, Burkhalter and Koschmieder<sup>8,9</sup> have also made a similar observation when investigating the stability of the Taylor–Couette flow in a small annulus, although the intent of their work was not aimed at the effect of acceleration. To distinguish it from the basic TVF, they refer to the extended TVF region as supercritical TVF.

As for the effect of aspect ratios, the results are presented in Figs. 1(a)–1(d) for a fixed radius ratio of 0.803, with each flow state represented by a different symbol for each data point, and the transition boundaries are indicated by “hatched” lines to account for the experimental uncertainty in locating their exact positions. In all cases, the radial diffusion time ( $d^2/\nu$ ) is 32.6 s. It is obvious from Fig. 1 that a reduction in the aspect ratio leads to an increase in the range of existence of the STVF regime. Moreover, there exists some threshold acceleration for each aspect ratio, beyond which the STVF regime is independent of the acceleration. In the case of  $\Gamma=50.54$ , this corresponds to an acceleration time which happens to be the same order as the radial diffusion time. However, as the aspect ratio is decreased the threshold acceleration time also decreases.

It is worth noting at this point that Fig. 1 is reproduced from Fig. 1 of Ref. 1, except that the acceleration has been expressed nondimensionally in the present paper. Also, it is obvious that at low aspect ratios of 20 and 15 [see Figs. 1(c) and 1(d)] the region of existence of STVF regime has expanded so much that it has merged with the TVF regime at the critical Reynolds number. This finding suggests that the end effects could have exerted a considerable influence in suppressing the formation of wavy vortex at low aspect ratios. However, the suppression is not uniform across the entire acceleration range as is indicated by the uneven shift in

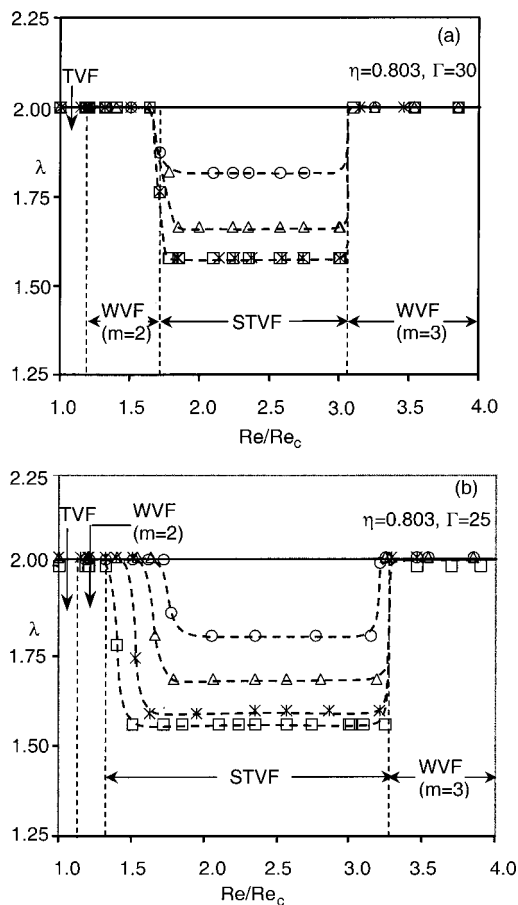


FIG. 2. Axial wavelength vs Reynolds number for different acceleration (a)  $\eta=0.803, \Gamma=30$ . (b)  $\eta=0.803, \Gamma=25$ .  $\circ$ :  $d Re/dt^*=598$ ,  $\triangle$ :  $d Re/dt^*=1196$ ,  $*$ :  $d Re/dt^*=3.59 \times 10^4$ ,  $\square$ :  $d Re/dt^*=6.52 \times 10^4$ .

the right hand side of the STVF boundary in Figs. 1(c) and 1(d).

Besides the flow state transition, we also examine the effect of radius ratio and aspect ratio on the axial wavelength ( $\lambda$ ) of the Taylor vortices. Because of the end effects, the cell size along the column is not completely uniform, and therefore, a mean or average axial wavelength ( $\lambda = 2H/Nd$ ) is used to characterize the flow. Here,  $N$  is the axial wave number, obtained by counting the total number of vortices along the whole length of the fluid column. The mean axial wavelength is obtained by repeating the experiment at least 10 times, and the results are then averaged over the total number of realizations.

Because the STVF regime is found only in  $\eta=0.803$ ,

only the axial wavelength for this particular radius ratio is presented [see Fig. 2(a)]. Here, the upper and the lower boundaries of the STVF regime are represented by two vertical broken lines, although in reality they are curved since they are dependent on both the acceleration and the Reynolds number. As Fig. 2(a) clearly shows, the axial wavelength ( $\lambda$ ) in the STVF regime for all accelerations is smaller than that in TVF and WVF regime (i.e.,  $\lambda \approx 2$ ), and decreases with increasing acceleration. For the two highest accelerations (i.e.,  $d Re/dt^*=3.59 \times 10^4$ , and  $d Re/dt^*=6.52 \times 10^4$  for sudden start), the data collapses on top of each other, which obviously suggests that the axial wavelength is independent of acceleration above some critical value. Increasing the aspect ratio of 50.54 does not change the trend of the results significantly, and the data for the two highest acceleration conditions still collapse on top of each other (see Ref. 7). At  $\Gamma \approx 25$ , the trend of the results still remains intact [see Fig. 2(b)], but there is a small region inside the STVF regime and in the vicinity of the TVF/STVF boundary that the axial wavelength is identical to that of TVF (i.e.,  $\lambda \approx 2$ ). This region grows in extent with decreasing aspect ratio, and when  $\Gamma \leq 20$ , the entire STVF regime is occupied by axisymmetric Taylor vortices of  $\lambda \approx 2$  (see Ref. 7) and is independent of the acceleration and Reynolds number. Interestingly, for the three higher aspect ratio cases (i.e.,  $\Gamma=25, 30$ , and  $50.54$ ), the axial wavelength for  $d Re/dt^*=598$  is  $\approx 1.8$  for all cases.

In summary, we have shown that the existence of STVF regime is sensitive to changes in the radius ratio and aspect ratio, and that the axial wavelength in the STVF regime is lower than in TVF and WVF for large aspect ratio, and the same as in TVF and WVF for low aspect ratio.

<sup>1</sup>T. T. Lim, Y. T. Chew, and Q. Xiao, "A new flow regime in a Taylor–Couette flow," *Phys. Fluids* **10**, 3233 (1998).  
<sup>2</sup>J. A. Cole, "Taylor-vortex instability and annulus-length effects," *J. Fluid Mech.* **75**, 1 (1976).  
<sup>3</sup>J. P. Holman, *Experimental Methods for Engineers*, 5th ed. (McGraw-Hill, New York, 1989).  
<sup>4</sup>G. I. Taylor, "Stability of a viscous liquid contained between two rotating cylinders," *Philos. Trans. R. Soc. London, Ser. A* **223**, 289 (1923).  
<sup>5</sup>R. C. DiPrima, P. M. Eagles, and B. S. Ng, "The effect of radius ratio on the stability of Couette flow and Taylor vortex flow," *Phys. Fluids* **27**, 2403 (1984).  
<sup>6</sup>W. Debler, E. Fünler, and B. Schaaf, "Torque and flow patterns in supercritical circular Couette flow," in *Proceedings of the 12th International Congress, Applied Mechanics*, edited by M. Hetényi and W. G. Vincenti (Springer, Berlin, 1969), p. 158.  
<sup>7</sup>Q. Xiao, Ph.D. thesis, National University of Singapore, 2000.  
<sup>8</sup>J. E. Burkhalter and E. L. Koschmieder, "Steady supercritical Taylor vortex flow," *J. Fluid Mech.* **58**, 547 (1973).  
<sup>9</sup>J. E. Burkhalter and E. L. Koschmieder, "Steady supercritical Taylor vortices after sudden starts," *Phys. Fluids* **17**, 1929 (1974).